Theoretical Study of the Operation and Performance of a Terahertz Quantum Cascade Laser Using Density Matrix Method

Mohd Asmu'i Mohd Akil[1,*], Amiruddin Shaari[1], Khalid Akabli[2], Mohd Khalid Kasmin[1] and Zulkafli Othaman[1]

[1]*Department of Physics, Faculty of Science, Universiti Teknologi Malaysia, 81310 Skudai, Johor, Malaysia*
[2]*Docteur En Physique Theorique Et Modelisation, France*

** asmuibakil@gmail.com*

(Received: 3 May 2016; published 11 Sept 2016)

Abstract. Terahertz (THz) quantum cascade lasers (QCL) are currently increasing its popularity in optoelectronic applications. It is expected to become the main source of emerging terahertz radiation technology and applications. However to produce the device within the application specification is costly and time consuming. Thus a prediction tool is needed to overcome the problems faced in designing and producing THz QCL within the required optical emission. The density matrix method is used to calculate the electronic and optical properties such as population density, current-voltage (I-V) and gain curves of this device. The results from this study were compared to the experimental ones conducted by previous researchers. From the calculation, the value of the gain is 20 cm^{-1} when the population inversion occurs starting from 400 A cm^{-2}. Meanwhile the loss occurs below 320 A cm^{-2}. As a conclusion, it is demonstrated that this method has the capability to explain the operation as well as to predict the performance of the THz QCL device.

Keywords: Terahertz source, density matrix, quantum cascade laser.

I. INTRODUCTION

The terahertz (THz) band is the part of electromagnetic spectrum located between photonic and electronic regions. It is a safe and harmless radiation because of its non-ionizing characteristic. It can penetrate into most materials, but not into water or metal. It promises many advantages over broad areas, especially in the field of security [1, 2, 3], spectroscopy [4, 5, 6] and medical imaging applications [7]. One of the promising THz radiation sources is a quantum cascade laser (QCL) [8, 9]. It is different from a conventional diode laser which operates through the recombination process between electrons and holes. THz QCL on the other hand operates by injecting electrons in to the device and these electrons are cascaded through a series of conduction bands in a superlattice of the device.

THz QCL is an excellent device because of its performance to produce high optical output power with narrow emission linewidth and of its small size. The output characteristics of this device can also be designed to fulfil specific requirements of applications by engineering the bandstructure of QCL system. Despite its advantages over other THz sources, improvement on the device design still poses a challenging task as the working principle of this device involves

many-body quantum physics. Therefore, a computational work is needed when designing the device to predict the performance of the device and thus to help making the cost of manufacturing of the device cheaper.

There are still some fundamental issues related to the working mechanism of THz QCL at microscopic levels that need some attention, in particular the role of the times of relaxation. They are known to affect the transport process inside the device, thus, critically affect the performance of the device. Insufficient study and analysis on the electronic transport in THz QCL can lead to an unlasing device which makes the whole work and time spent in fabricating and testing the device a waste. A density matrix method can be used to study the electronic transport in QCL to estimate or predict the electrical characteristics of its output as well as its optical performance based on light-current-voltage (L-I-V) profile. This should lead to a better understanding of the system as the method explicitly incorporates the effects of the electronic transitions responsible for the population inversion and the actual laser emission.

The theoretical work to analyse the properties of the superlattice structure was pioneered by Kazarinov and Suris [10] utilizing numerical analysis. Then, the density matrix method was applied to study the transport properties of quantum cascade laser. In the present research, the density matrix method for THz QCL is improved by incorporating the effects of scattering inside the device in particular the effects of the times of relaxation. This enhancement allows, the population density of a particular level whenever it is populated or depopulated, to be determined. The results discussed and presented in this article are generated from a computational work on a THz QCL design similar to the one studied experimentally by Kumar et al. [11]. The device simulated in this work is a four-level resonant tunneling THz QCL made of layers of AlGaAs (barriers) and GaAs (wells). The purpose of this study is to model the device operation and performance using the density matrix method and to determine the required parameters to achieve population inversion to support laser emission. This study also generates the current-voltage (I-V) characteristic, population density and finally the gain for the device.

II. METHODOLOGY

There are several widely used THz QCL designs such as the bound-to-continuum, the chirped superlattice and resonant phonon [12]. Each THz QCL design has its own mechanism of operation. In this study, we use resonant phonon THz QCL design. It is called a resonant phonon design because it utilizes the longitudinal optical (LO)-phonon resonance as the mechanism to depopulate the lower state of the laser and at the same time to inject the current to the adjacent upper level. The system used for the calculation described in this paper is a 4-level system as shown in Figure 1.

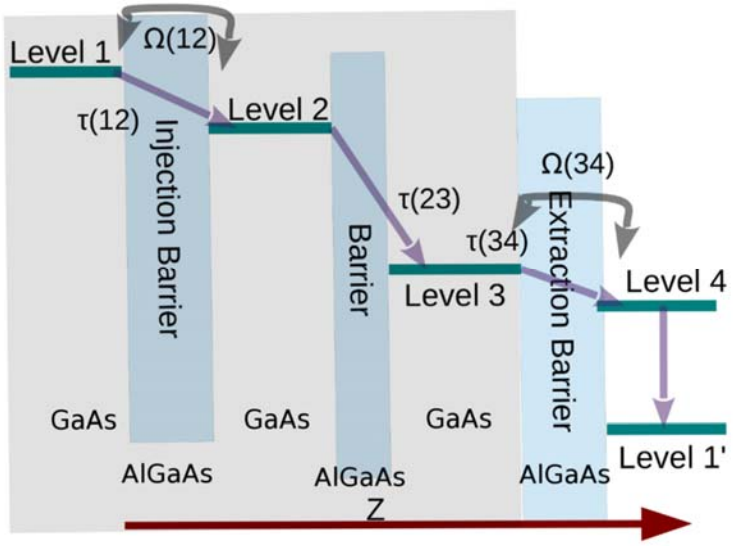

FIGURE 1. Schematic representation one period of a 4-level system [5] under bias voltage. The shaded region represent one period of the THz QCL structure.

The period consists of the first GaAs layer where the extraction level of adjacent period and the injector (level 1) are located, an AlGaAs layer as the injection barrier, the second GaAs layer where upper level (level 2) is located, an AlGAs layer as middle barrier, third GaAs layer where lower level (level 3) is located, and AlGaAs as an extraction barrier. These periods are repeated on both sides to form the active regions to produce laser. THz QCL usually consists of more than 100 periods. The electronic performance of the QCL device is investigated through the electrical current produced by the device. The current considered in this calculation is due to the electrons transported from one energy level to the neighbouring energy level. The THz radiation is produced by the transition between level 2 and level 3. The depopulation of level 4 to level 1' occurs via non-radiative transition via longitudinal optical (LO) phonon resonance. For a laser system based on GaAs, this LO-phonon has an energy of 36 meV [13].

The optical performance of the laser is investigated through its optical gain. The optical gain of a laser is defined as a relative increase of electromagnetic wave intensity per unit length as the wave propagates through the active medium [14, 15, 16]. In THz QCL, the gain comes from photons generated by laser emission in the active region within supported optical modes of the laser waveguide. Experimentally, the THz QCL gain can be measured by time domain spectroscopy [17]. Performance of THz QCL device operating at high temperature depends strongly on its gain, which can be calculated and analysed only if the current-vontage, I-V characteristic curve of the device is known.

The analysis of the four-level system using density matrix method in this work follows the same procedures as described by other researchers [18, 19, 20, 21] working on a three-level system with a few improvements. The density matrix ρ is used to represent the state of the system in which the diagonal elements (ρ_{ii}) show the population of individual state and the off-diagonal elements (ρ_{ij}) show the coherence between them.

The equation of motion or the time evolution of the density matrix of the system is written as:

$$\frac{d\rho}{dt} = -\frac{i}{\hbar}[H, \rho] \tag{1}$$

where $H = H_0 + H'$, is the total Hamiltonian of the system, H_0 and H' are called the unperturbed and the perturbation parts of the total Hamiltonian respectively and [,] represent the commutator between two operators. Thus, the time of evolution of the density matrix in terms of H_0 and H' can then be written as:

$$\frac{d\rho}{dt} = -\frac{i}{\hbar}([H_0, \rho] + [H', \rho]) \tag{2}$$

and each commutator can be explicitly expanded as :

$$[H_0, \rho] = \left[\begin{pmatrix} E_1 & \hbar\Omega_{12} & \hbar\Omega_{13} & \hbar\Omega_{14} \\ \hbar\Omega_{12} & E_2 & \hbar\Omega_{23} & \hbar\Omega_{24} \\ \hbar\Omega_{13} & \hbar\Omega_{23} & E_3 & \hbar\Omega_{34} \\ \hbar\Omega_{14} & \hbar\Omega_{24} & \hbar\Omega_{34} & E_4 \end{pmatrix} \begin{pmatrix} \rho_{11} & \rho_{12} & \rho_{13} & \rho_{14} \\ \rho_{21} & \rho_{22} & \rho_{23} & \rho_{24} \\ \rho_{31} & \rho_{32} & \rho_{33} & \rho_{34} \\ \rho_{41} & \rho_{42} & \rho_{43} & \rho_{44} \end{pmatrix} \right] \tag{3}$$

where E_i and Ω_{ij} are the eigenenergies and Rabi frequencies between two energy levels

$$\frac{i}{\hbar}[H', \rho] = \begin{bmatrix} \tau_1^{-1}\rho_{11} - \tau_4^{-1}\rho_{44} & \tau_{12}^{-1}\rho_{12} \\ \tau_{12}^{-1}\rho_{21} & \tau_2^{-1}\rho_{22} - \tau_3^{-1}\rho_{33} + \tau_{st}^{-1}\Delta\rho \\ \tau_{13}^{-1}\rho_{31} & \tau_{23}^{-1}\rho_{32} \\ \tau_{14}^{-1}\rho_{41} & \tau_{24}^{-1}\rho_{42} \end{bmatrix}$$

$$\begin{bmatrix} \tau_{13}^{-1}\rho_{13} & \tau_{14}^{-1}\rho_{14} \\ \tau_{23}^{-1}\rho_{23} & \tau_{24}^{-1}\rho_{24} \\ -\tau_2^{-1}\rho_{22} + \tau_3^{-1}\rho_{33} - \tau_{st}^{-1}\Delta\rho & \tau_{34}^{-1}\rho_{34} \\ \tau_{34}^{-1}\rho_{43} & -\tau_1^{-1}\rho_{11} + \tau_4^{-1}\rho_{44} \end{bmatrix} \tag{4}$$

where τ_{ij} are the times of relaxation, $\Delta\rho = \rho_{22} - \rho_{33}$ is the population inversion, and *st* is an abbreviation for stimulated transition. All of the Rabi oscillation frequencies and time relaxation parameters, τ in perturbation H' are as described by Callebaut and Hu [22].

In this method all the difficulties in the analysis are hidden behind the terms related to the relaxation times which are often regarded as phenomenological terms. The average current density in A cm^{-2} is calculated using expression, $j = eTr\ [\upsilon\rho]$, where e is the charge of an electron, Tr trace operation of a matrix, υ the velocity and ρ the density operator. The velocity operator in turn can be written as $\upsilon = i/\hbar\ [H, Z]$, Z is the position operator and $\hbar$ is the planck constant. Thus the average current density can be determined from equation:

$$j = e\frac{i}{\hbar}Tr\left[\left[H,Z\right]\rho\right] \tag{5}$$

A current-voltage (I-V) profile can be achieved by calculating the average current density j with respect to the bias voltage, V which is set as a parameter when solving the rate equation above. Bear in mind the bias voltage V is part of the Hamiltonian H used in solving the envelope wavefunctions for the electrons in the active region.

The time evolution of the population densities during the laser emission is calculated by solving the following equations:

$$\frac{d\rho_{22}}{dt} = \frac{j}{e} - \rho_{22}\tau_2^{-1} - \sigma\Gamma S\left(\rho_{22} - \rho_{33}\right) \tag{6}$$

$$\frac{d\rho_{33}}{dt} = -\rho_{33}\tau_3^{-1} - \sigma\Gamma S\left(\rho_{33} - \rho_{22}\right) + \rho_{22}\tau_{23}^{-1} \tag{7}$$

$$\sigma = \frac{4\pi e^2}{\varepsilon_0 n} * \frac{\left|\mu_{23}\right|^2}{\lambda} * \frac{c}{n} * \frac{1}{L_v 2\gamma_{23}} \tag{8}$$

where S is the photon surface density in m^{-2}, Γ is the overlap factor between the optical mode and the active region of the waveguide in percent, ε_0 is the vacuum permittivity at $8.854\cdot10^{-12}$ As V^{-1} m^{-1}, γ_{23} is the full width half maximum (FWHM) of the spontaneous emission line in s. The rate of photon surface density is represent as :

$$\frac{dS}{dt} = \sigma\Gamma S\left(\rho_{22} - \rho_{33}\right) - \frac{c}{n}\alpha S \tag{9}$$

where α is the total losses in m^{-1}, μ is the element of dipole matrix in m, σ is the cross section area per unit time in m^2 s^{-1}, c is the speed of light in ms^{-1}, λ is the wavelength of laser in m, n is the refractive index of the medium, e is the charge of electron and L_p is the length of a period in m. Finally, the gain is calculated by using the following equation :

$$Gain = \sigma n\left(\rho_{22} - \rho_{33}\right)\frac{n_{tot}}{c} \tag{10}$$

where n_{tot} is the total number of electrons per period.

III. RESULTS AND DISCUSSIONS

The model is tested against an established resonant phonon THz QCL design studied by Kumar [11]. This design consists of four levels namely the injector (level 1), upper level (level 2), lower level (level 3) and extractor level (level 4) and has 222 active region periods. Figure 2 shows the bandstructure of one period of the active region (grey) together with squared modulus

of the envelope wavefunctions representing the probability density of finding the electrons in the quantum wells.

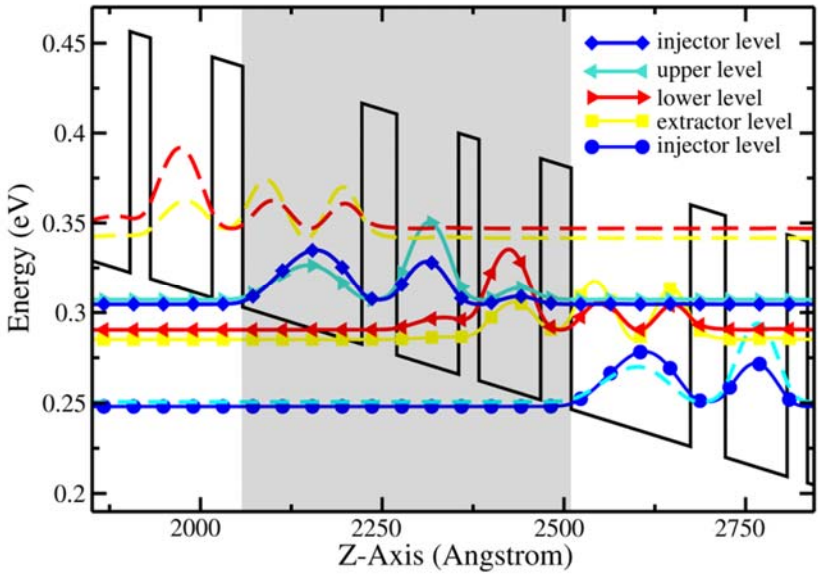

FIGURE 2. Conduction band diagram for a four levels THz QCL system at 18kV/cm operating bias with the layer thicknesses 16.4/**4.8**/8.5/**2.8**/8.5/**4.2**, (bold fonts indicate the barriers and the unit is in nm). The shaded region represent one period of the THz QCL structure.

The THz QCL structure comprises several $Al_xGa_{1-x}As$ and GaAs layers sandwiched side by side. The geometry and dimension of THz QCL structure used in this calculation allow a study of the parasitic current occurring between the injector and extractor level. This study assumes possible resonant tunneling process between the injector and the upper level and between the injector and the lower level by the interface roughness. The photon emission is due to transition between the 2-3 level (upper to lower level) and the relaxation from the extractor to the next injector level using an LO-phonon resonance.

Hence, by solving the Hamiltonian in all the levels inside the equation of motion, Figure 3 is obtained. The figure shows the evolution of population density in injector level, upper level, lower level and extractor level with the changing of the bias voltage. By referring to upper level in this figure, the population inversion occurs at bias voltage about 10.75 V.

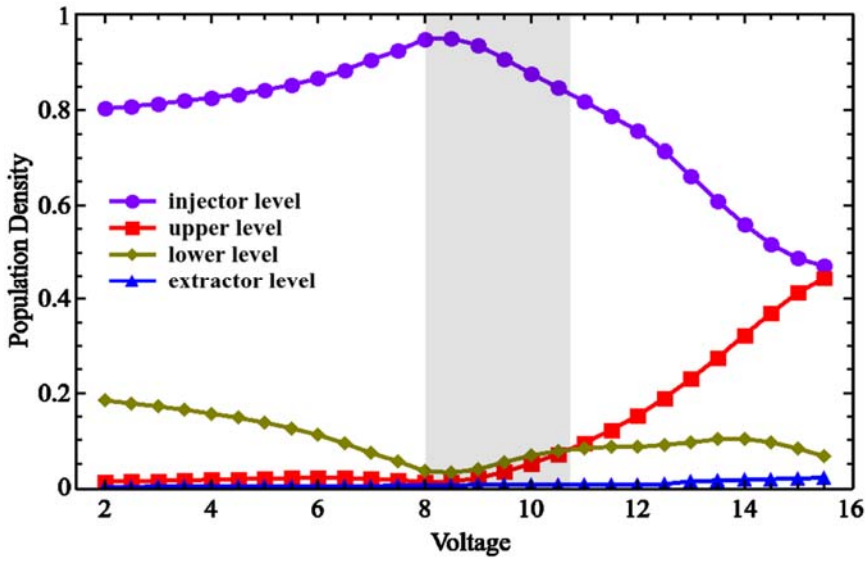

FIGURE 3. The evolution of population density in injector, upper, lower and extraction level by the evolution of bias, in Volt.

The population of the injector level then start to decrease at about 8.5 V, meanwhile the populations of the upper level increase. The population inversion occurs when the upper level is highly populated than the lower level. The population in injector level increases with the bias voltage change until the levels are aligned which is the condition for the electrons to tunnel through barrier. For this inversion to occur, a good extraction mechanism is needed at the lower level to make the level always in "vacancy". If not, it will destroy the population inversion of the laser. Thus the mechanism to depopulate the lower level is by using the LO-phonon resonance, the electron transition from lower level to the injector level into the adjacent period.

Finally, by solving the equations (1) to (5), the calculated I-V is plotted as shown in Figure 4 along with the experimental I-V curve. Referring to Figure 4, the calculated I-V has almost the same pattern with the experimental result. There are few assumptions made in this calculation such as the use of a tight-binding basis, population relaxation due to LO-phonon resonance and interface roughness scattering at the device temperature ~ 0 K, whereas for the experimental result is at 9 K. That is the reason why the calculated trendline for I-V curve shows some deviation from the experimental one.

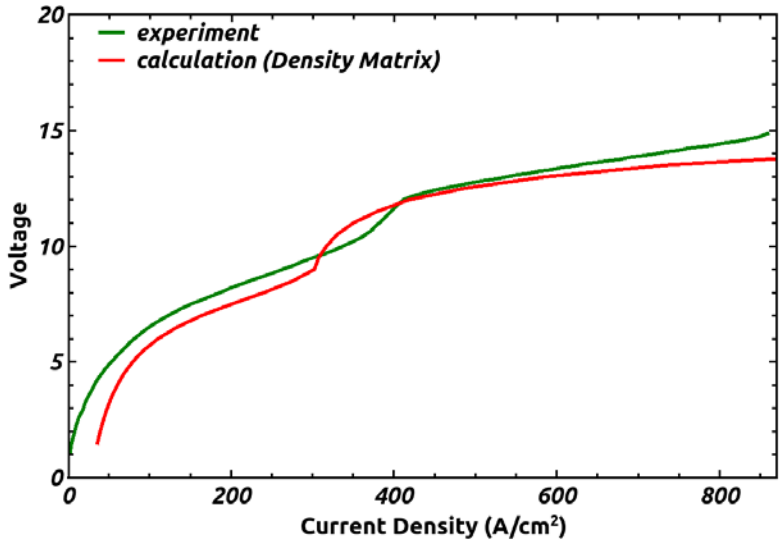

FIGURE 4. Curve extracted from Kumar [11] and the calculated result using the density matrix method.

The THz radiation produced by the laser depends on the energy difference between upper and lower level (level 2 and 3). In the calculation, as the bias voltage is changed from about 0 V to 12 V the laser achieves population inversion and THz radiation is produced. The frequency of the terahertz radiation produced by the device changes as the bias voltage is changed. The dependence of the optical performance of the device on the terahertz frequency usually is depicted by its gain profile. Figure 5 shows the gain evolution as the current density changes.

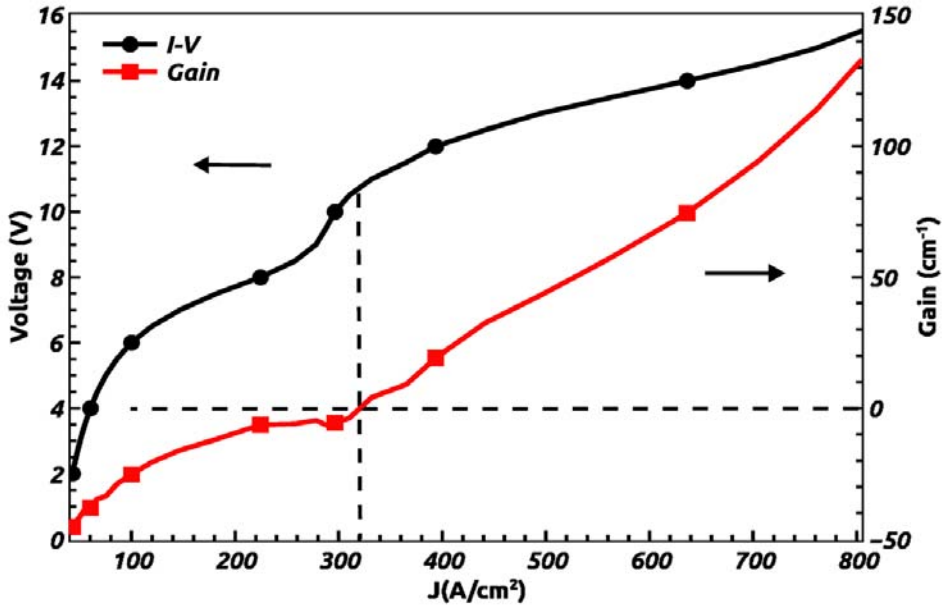

FIGURE 5. The calculated I-V using density matrix method and the calculated evolution of the gain for THz QCL with the change of current density.

At the current density of about 320 A cm^{-2}, the value of gain is 0 cm^{-1}, this is the starting point for the population inversion process. Below this current density, there is no emission produced by this THz QCL and the gain during this phase is negative. As the current density approaches the value of 400 A cm^{-2}, the threshold current density is achieved for the device to start laser emission. At this current density, the population inversion is stable enough for laser production because of the transition from upper level to lower level and then to extraction level. The electrons in extraction level are being depopulated using LO-phonon to the next injector level. This process goes on through the entire active region. From this study, even though the population inversion starts at 320 A cm^{-2}, but the transition responsible for laser emission only occurs after 400 A cm^{-2}. The current density for transition of electrons to produce laser turns out not at the same current density of the starting of the population inversion process. This is because during the starting of population inversion, the levels in this system are not aligned properly for the requirement to produce a transition to make laser emission. The level aligns properly and meets the requirement for laser transition at 400 A cm^{-2} which produces a gain value of about 20 cm^{-1}.

IV. CONCLUSIONS

From this study, a prediction tool based on density matrix method which enables the computation of the current-voltage (I-V) and optical gain of THz QCL has been successfully developed. Although, the predicted I-V and gain for QCL are considered good and exhibit similar patterns compared to those from the experimental results [23], the model itself is far from perfection. This is mainly due to the approximations assumed in the calculation namely the exclusion of the surface roughness and the values of times of relaxation. Further improvement can be made to this method by including the effects of coherences and other times of relaxation as well as the effect of temperature to the device.

Acknowledgements

The authors would like to acknowledge financial support from Fundamental Research Grant Scheme (vot. No. R.J130000.7826.4F244) from Ministry of Education and Universiti Teknologi Malaysia.

---

1. W. H. Fan, A. Burnett, P. C. Upadhya, J. Cunningham, E. H. Linfield, and a G. Davies, *Appl. Spectrosc*. **61**, 638 (2007).
2. A. D. Burnett, W. Fan, P. C. Upadhya, J. E. Cunningham, M. D. Hargreaves, T. Munshi, H. G. M. Edwards, E. H. Linfield, and a G. Davies, *Analyst* **134**, 1658 (2009).
3. M. R. Leahy-Hoppa, M. J. Fitch, and R. Osiander, *Anal. Bioanal. Chem.* **395**, 247 (2009).
4. P. U. Jepsen, D. G. Cooke, and M. Koch, *Laser Photon. Rev.* **5**, 124 (2011).
5. H.-W. Hübers, R. Eichholz, S. G. Pavlov, and H. Richter, *J. Infrared, Millimeter, Terahertz Waves* **34**, 325 (2013).
6. Y. Wang, M. G. Soskind, W. Wang, and G. Wysocki, *Appl. Phys. Lett.* **104**, 031114 (2014).

7. M. Tonouchi, *Nat. Photonics* **1**, 97 (2007).
8. J. Faist, F. Capasso, D. Sivco, and C. Sirtori, *Science*. **264**, 553 (1994).
9. R. Kohler, a Tredicucci, F. Beltram, H. Beere, E. Linfield, G. Davies, D. Ritchie, R. Iotti, and F. Rossi, *Phys. Semicond.* 2002, Proc. **171**, 145 (2003).
10. R. F. Kazarinov and R. A. Suris, *Sov. Phys. - Semicond.* **5**, 707 (1971).
11. S. Kumar, Q. Hu, and J. L. Reno, *Appl. Phys. Lett.* **94**, (2009).
12. B. S. Williams, *Nat. Photonics* **1**, 517 (2007).
13. D. Strauch and B. Dorner, *J. Phys. Condens. Matter* **2**, 1457 (1999).
14. F. Banit, S. C. Lee, A. Knorr, and A. Wacker, *Appl. Phys. Lett.* **86**, (2005).
15. M. Martl, J. Darmo, C. Deutsch, M. Brandstetter, A. M. Andrews, P. Klang, G. Strasser, and K. Unterrainer, *Opt. Express* **19**, 733 (2011).
16. R. Nelander and A. Wacker, *Appl. Phys. Lett.* **92**, (2008).
17. N. Jukam, S. S. Dhillon, D. Oustinov, Z.-Y. Zhao, S. Hameau, J. Tignon, S. Barbieri, a. Vasanelli, P. Filloux, C. Sirtori, and X. Marcadet, *Appl. Phys. Lett.* **93**, 101115 (2008).
18. S. Kumar and Q. Hu, *Phys. Rev. B - Condens. Matter Mater. Phys.* **80**, (2009).
19. R. Köhler, R. C. Iotti, A. Tredicucci, and F. Rossi, *Appl. Phys. Lett.* **79**, 3920 (2001).
20. R. Terazzi and J. Faist, *New J. Phys.* **12**, 033045 (2010).
21. E. Dupont, S. Fathololoumi, and H. C. Liu, *Phys. Rev. B - Condens. Matter Mater. Phys.* **81**, (2010).
22. H. Callebaut and Q. Hu, *J. Appl. Phys.* **98**, (2005).
23. S. Kumar, Q. Hu, and J. L. Reno, *Appl. Phys. Lett.* **94**, 131105 (2009).